



HAL
open science

Optimal choice of Hankel-block-Hankel matrix shape in 2-D parameter estimation

Souleymen Sahnoun, Konstantin Usevich, Pierre Comon

► **To cite this version:**

Souleymen Sahnoun, Konstantin Usevich, Pierre Comon. Optimal choice of Hankel-block-Hankel matrix shape in 2-D parameter estimation. [Research Report] GIPSA-lab. 2016. hal-01288994v1

HAL Id: hal-01288994

<https://hal.science/hal-01288994v1>

Submitted on 15 Mar 2016 (v1), last revised 6 Jul 2016 (v2)

HAL is a multi-disciplinary open access archive for the deposit and dissemination of scientific research documents, whether they are published or not. The documents may come from teaching and research institutions in France or abroad, or from public or private research centers.

L'archive ouverte pluridisciplinaire **HAL**, est destinée au dépôt et à la diffusion de documents scientifiques de niveau recherche, publiés ou non, émanant des établissements d'enseignement et de recherche français ou étrangers, des laboratoires publics ou privés.

Optimal choice of Hankel-block-Hankel matrix shape in 2-D parameter estimation

Souleymen Sahnoun, Konstantin Usevich, Pierre Comon

Abstract—In this paper we analyse the performance of 2-D ESPRIT method for estimating parameters of 2-D superimposed damped exponentials. 2-D ESPRIT algorithm is based on low-rank decomposition of a Hankel-block-Hankel matrix that is formed by the 2-D data. Through a first-order perturbation analysis, we derive expressions of the variance of the estimates in 2-D multiple-tones case. We also derive closed-form expressions of the variances of the complex modes, frequencies and damping factors estimates in the 2-D single-tone case. This analysis allows to define the optimal parameters used in the construction of the Hankel-block-Hankel matrix. A fast algorithm for calculating the SVD of Hankel-block-Hankel matrices is also used to enhance the computational complexity of the 2-D ESPRIT algorithm.

Index Terms—Frequency estimation, Hankel-block-Hankel matrix, 2-D ESPRIT, perturbation analysis.

I. INTRODUCTION

High resolution parameter estimation of bidimensional (2-D) and multidimensional signals finds many applications in sensor array processing, such as radar, wireless communications, sonar, seismology, or medical imaging.

a) State of art: To deal with this problem, several parametric methods have been proposed. They include linear prediction-based methods such as 2-D TLS-Prony [1], and subspace approaches such as matrix enhancement and matrix pencil (MEMP) [2], 2-D ESPRIT [3], multidimensional folding (MDF) [4], improved multidimensional folding (IMDF) [5], [6], and the methods proposed in [7]–[9]. It is generally admitted that these methods yield accurate estimates at high SNR and/or when the frequencies are well separated. Statistical performances of some of these methods have been studied in the case of undamped sinusoids [5], [6]. Recently, analytical performances of tensor-based ESPRIT-type algorithms have been assessed for undamped signals [10].

In this paper, we focus our attention on the 2-D ESPRIT algorithm of [3]. In sensor array processing, this approach can be used to address the case of a single snapshot via spatial smoothing [7]. The performance of 2-D ESPRIT depends on the shape of the Hankel-block-Hankel (HbH) matrix constructed from 2-D data. To our knowledge, no theoretical study has yet been conducted (especially for damped signals) to optimally choose parameters defining the HbH matrix.

b) Contributions: The main contribution consists in the derivation of closed-form expressions of the variance of the complex modes, frequencies and damping factors estimates in case of 2-D damped single-tone signals. These expressions are

used to define the optimal size of the sub-windows used in the construction of the HbH matrix. We also derive expressions of first-order perturbations of the parameters in the multiple tone case. Finally, we propose to use a fast algorithm to compute the SVD of the HbH matrix, which reduces the computational complexity of 2-D ESPRIT for large signals.

c) Organisation of the paper: In Section II, we introduce notation, present the 2-D modal retrieval problem and recall the 2-D ESPRIT algorithm. In Section III, a first-order perturbation analysis for 2D-ESPRIT is performed. In Section IV, the single tone case is analyzed and the optimal parameters for the construction of the HbH matrix are discussed. In Section V, computer results are presented to verify the theoretical expressions. We also discuss the complexity of the SVD.

II. PARAMETER ESTIMATION USING 2-D ESPRIT

The classical model for 2-D modal signals is the superposition of 2-D damped complex sinusoids in noise. In other words, we observe:

$$\tilde{y}(m_1, m_2) = \sum_{r=1}^R c_r a_r^{m_1} b_r^{m_2} + e(m_1, m_2) \quad (1)$$

for $m_1 = 0, \dots, M_1 - 1$ and $m_2 = 0, \dots, M_2 - 1$, where $a_r = e^{-\alpha_{a,r} + j\omega_{a,r}}$ are the modes of the first dimension and $b_r = e^{-\alpha_{b,r} + j\omega_{b,r}}$ are those of the second dimension. $\{\alpha_{a,r}, \alpha_{b,r}\}_{r=1}^R$ are damping factors, $\{\omega_{a,r} = 2\pi\nu_{a,r}\}_{r=1}^R$ and $\{\omega_{b,r} = 2\pi\nu_{b,r}\}_{r=1}^R$ are angular frequencies and $\{c_r\}_{r=1}^R$ are complex amplitudes; $e(m_1, m_2)$ is a zero-mean complex Gaussian white noise with variance σ_e^2 and mutually independent components in all dimensions. The problem is to estimate $\{a_r, b_r, c_r\}_{r=1}^R$ from the observed signal $\tilde{y}(m_1, m_2)$. In this paper, the tilde ($\tilde{\cdot}$) denotes a noisy signal.

A. 2-D ESPRIT algorithm

Define the HbH matrix

$$\mathbf{H} = \begin{bmatrix} \mathbf{H}_0 & \mathbf{H}_1 & \dots & \mathbf{H}_{K_1-1} \\ \mathbf{H}_1 & \mathbf{H}_2 & \dots & \mathbf{H}_{K_1} \\ \vdots & \vdots & \ddots & \vdots \\ \mathbf{H}_{L_1-1} & \mathbf{H}_{L_1} & \dots & \mathbf{H}_{M_1-1} \end{bmatrix}, \quad (2)$$

where each block \mathbf{H}_{m_1} is an $L_2 \times K_2$ Hankel matrix

$$\mathbf{H}_{m_1} = \begin{bmatrix} y(m_1, 0) & y(m_1, 0) & \dots & y(m_1, K_2-1) \\ y(m_1, 1) & y(m_1, 2) & \dots & y(m_1, K_2) \\ \vdots & \vdots & \ddots & \vdots \\ y(m_1, L_2-1) & y(m_1, L_2) & \dots & y(m_1, M_2-1) \end{bmatrix} \quad (3)$$

for $m_1 = 0, \dots, M_1 - 1$. We shall also denote $\tilde{\mathbf{H}}$ and $\tilde{\mathbf{H}}_{m_1}$ the noisy versions built upon noisy observations $\tilde{y}(m_1, m_2)$. Then 2-D ESPRIT algorithm [3] can be summarized as follows:

This work is funded by the European Research Council under the Seventh Framework Programme FP7/2007–2013 Grant Agreement no. 320594.

S. Sahnoun, K. Usevich and P. Comon are with CNRS, Gipsa-Lab, F-38000 Grenoble, France (e-mail: firstname.name@gipsa-lab.grenoble-inp.fr).

- Choose L_1, L_2 and set $K_1 = M_1 - L_1 + 1, K_2 = M_2 - L_2 + 1$.
- Construct the HbH matrix $\tilde{\mathbf{H}}$ with $L_1 \times K_1$ blocks, in the same format as in (2). It can be verified that its noiseless part can be written as

$$\mathbf{H} = \left(\mathbf{A}^{(L_1)} \odot \mathbf{B}^{(L_2)} \right) \text{Diag}(\mathbf{c}) \left(\mathbf{A}^{(K_1)} \odot \mathbf{B}^{(K_2)} \right)^{\top} \quad (4)$$

where \odot denotes the Khatri-Rao product, $\mathbf{A}^{(P)}$ (resp. $\mathbf{B}^{(P)}$) denotes the Vandermonde matrix with P rows and R columns, containing coefficients a_r^p (resp. b_r^p), $p \in \{0, \dots, P-1\}$, and $\text{Diag}(\mathbf{c})$ is a diagonal $R \times R$ matrix containing coefficients c_r .

- Perform the SVD of $\tilde{\mathbf{H}}$, and form the matrix $\mathbf{U}_s \in \mathbb{C}^{L_1 L_2 \times R}$ of the R dominant singular vectors.
- Compute the matrices \mathbf{F}_1 et \mathbf{F}_2 such that:

$$\mathbf{F}_1 = (\mathbf{U}_s)^\dagger \tilde{\mathbf{U}}_s, \quad \mathbf{F}_2 = (\mathbf{U}_s)^\dagger \tilde{\mathbf{U}}_s, \quad (5)$$

where (\dagger) denotes the pseudoinverse, and for a matrix

$$\mathbf{X} = \begin{bmatrix} \mathbf{x}_1 \\ \vdots \\ \mathbf{x}_{L_1} \end{bmatrix} \in \mathbb{C}^{L_1 L_2 \times N}, \quad \text{with } \mathbf{x}_k \in \mathbb{C}^{L_2 \times N},$$

matrices $\tilde{\mathbf{X}}, \tilde{\mathbf{X}} \in \mathbb{C}^{(L_1-1)L_2 \times N}$, $\tilde{\mathbf{X}}, \tilde{\mathbf{X}} \in \mathbb{C}^{L_1(L_2-1) \times N}$ are defined as

$$\tilde{\mathbf{X}} = \begin{bmatrix} \mathbf{x}_1 \\ \vdots \\ \mathbf{x}_{L_1-1} \end{bmatrix}, \quad \tilde{\mathbf{X}} = \begin{bmatrix} \mathbf{x}_2 \\ \vdots \\ \mathbf{x}_{L_1} \end{bmatrix}, \quad \tilde{\mathbf{X}} = \begin{bmatrix} \mathbf{x}_1 \\ \vdots \\ \mathbf{x}_{L_1} \end{bmatrix}, \quad \tilde{\mathbf{X}} = \begin{bmatrix} \mathbf{x}_1 \\ \vdots \\ \mathbf{x}_{L_1} \end{bmatrix},$$

where \cdot (resp. $\bar{\cdot}$) removes the last (resp. first) row.

- Compute a diagonalizing matrix \mathbf{T} from a linear combination $\mathbf{K} = \beta \mathbf{F}_1 + (1-\beta) \mathbf{F}_2$ (β is a user parameter):

$$\mathbf{K} = \mathbf{T} \text{Diag}(\boldsymbol{\eta}) \mathbf{T}^{-1}. \quad (6)$$

- Apply the transformation \mathbf{T} to \mathbf{F}_1 and \mathbf{F}_2 :

$$\mathbf{D}_a = \mathbf{T}^{-1} \mathbf{F}_1 \mathbf{T} \quad \text{and} \quad \mathbf{D}_b = \mathbf{T}^{-1} \mathbf{F}_2 \mathbf{T}. \quad (7)$$

- Extract a_r, b_r from $\text{diag}(\mathbf{D}_a)$ and $\text{diag}(\mathbf{D}_b)$.

The 2-D ESPRIT method does not require a pairing step. Indeed, the (r, r) element of $\text{Diag}(\mathbf{a})$ corresponds to the same 2-D signal component as the (r, r) element of $\text{Diag}(\mathbf{b})$. Hence, 2-D ESPRIT can estimate the parameters in the presence of identical modes in the dimensions.

III. ANALYSIS OF THE 2-D ESPRIT METHOD

A. Perturbation of signal subspace \mathbf{U}_s

The SVD of the noiseless HbH matrix \mathbf{H} is given by:

$$\mathbf{H} = \mathbf{U}_s \boldsymbol{\Sigma}_s \mathbf{V}_s^{\text{H}} + \mathbf{U}_n \boldsymbol{\Sigma}_n \mathbf{V}_n^{\text{H}}$$

where $\boldsymbol{\Sigma}_n = \mathbf{0}$. The perturbed $\tilde{\mathbf{H}}$ is expressed as

$$\tilde{\mathbf{H}} = \mathbf{H} + \Delta \mathbf{H},$$

whose subspace decomposition is given by

$$\tilde{\mathbf{H}} = \tilde{\mathbf{U}}_s \tilde{\boldsymbol{\Sigma}}_s \tilde{\mathbf{V}}_s^{\text{H}} + \tilde{\mathbf{U}}_n \tilde{\boldsymbol{\Sigma}}_n \tilde{\mathbf{V}}_n^{\text{H}} \quad (8)$$

We use the following lemma on the first-order approximation.

Lemma 1 ([11] and [12]): The perturbed signal subspace is $\tilde{\mathbf{U}}_s = \mathbf{U}_s + \Delta \mathbf{U}_s$, $\tilde{\mathbf{V}}_s = \mathbf{V}_s + \Delta \mathbf{V}_s$ and $\tilde{\boldsymbol{\Sigma}}_s = \boldsymbol{\Sigma}_s + \Delta \boldsymbol{\Sigma}_s$. A first order approximation of the perturbation is given by

$$\Delta \mathbf{U}_s = \mathbf{U}_n \mathbf{U}_n^{\text{H}} \Delta \mathbf{H} \mathbf{V}_s \boldsymbol{\Sigma}_s^{-1} \quad (9)$$

$$\Delta \mathbf{V}_s^{\text{H}} = \boldsymbol{\Sigma}_s^{-1} \mathbf{U}_s^{\text{H}} \Delta \mathbf{H} \mathbf{V}_n \mathbf{V}_n^{\text{H}} \quad (10)$$

$$\Delta \boldsymbol{\Sigma}_s = \mathbf{U}_s^{\text{H}} \Delta \mathbf{H} \mathbf{V}_s \quad (11)$$

B. Perturbations of the matrices $\mathbf{F}_1, \mathbf{F}_2$ and \mathbf{K}

From (5), we have $\tilde{\mathbf{U}}_s \tilde{\mathbf{F}}_1 = \tilde{\mathbf{U}}_s$, which is written also as $(\mathbf{U}_s + \Delta \mathbf{U}_s)(\mathbf{F}_1 + \Delta \mathbf{F}_1) = (\tilde{\mathbf{U}}_s + \Delta \tilde{\mathbf{U}}_s)$. By canceling $\mathbf{U}_s \mathbf{F}_1$ and $\tilde{\mathbf{U}}_s$, and neglecting $\Delta \mathbf{U}_s \Delta \mathbf{F}_1$, we get

$$\Delta \mathbf{F}_1 = \mathbf{U}_s^\dagger (\Delta \tilde{\mathbf{U}}_s - \Delta \mathbf{U}_s \mathbf{F}_1) \quad (12)$$

Similarly, the first-order perturbation $\Delta \mathbf{F}_2$ is given by:

$$\Delta \mathbf{F}_2 = \mathbf{U}_s^\dagger (\Delta \tilde{\mathbf{U}}_s - \Delta \mathbf{U}_s \mathbf{F}_2) \quad (13)$$

and matrix \mathbf{K} defined in the previous section eventually takes the form: $\Delta \mathbf{K} = \beta \Delta \mathbf{F}_1 + (1-\beta) \Delta \mathbf{F}_2$.

C. Perturbations of the modes: the general case

First, we calculate perturbations of eigenvectors \mathbf{t}_r (the columns of matrix \mathbf{T}). After some simplifications, we get $\Delta \mathbf{t}_f = \sum_{i=1, i \neq r}^R \gamma_{ir} \mathbf{t}_i$ where

$$\gamma_{ir} = \frac{\boldsymbol{\tau}_i^{\text{T}} \Delta \mathbf{K} \mathbf{t}_r}{\lambda_r - \lambda_i}, \quad i \neq r$$

where $\mathbf{T}^{-1} \stackrel{\text{def}}{=} [\boldsymbol{\tau}_1, \dots, \boldsymbol{\tau}_R]^{\text{T}}$. Then we get

$$\Delta \mathbf{t}_r = \sum_{i=1, i \neq r}^R \frac{1}{\eta_r - \eta_i} \mathbf{t}_i \boldsymbol{\tau}_i^{\text{T}} \Delta \mathbf{K} \mathbf{t}_r \quad (14)$$

$$= \mathbf{T} \boldsymbol{\Xi}(r) \mathbf{T}^{-1} \Delta \mathbf{K} \mathbf{t}_r \quad (15)$$

where $\boldsymbol{\Xi}(r)$ is a diagonal matrix with $\boldsymbol{\Xi}_{ii}(r) = \frac{1}{\eta_r - \eta_i}$, for $i \neq r$ and $\boldsymbol{\Xi}_{rr}(r) = 0$. Finally, the perturbations of the mode estimates is computed using (7)

$$\begin{cases} \Delta a_r = \boldsymbol{\tau}_r^{\text{T}} ((a_r \mathbf{I} - \mathbf{F}_1) \Delta \mathbf{t}_r - \Delta \mathbf{F}_1 \mathbf{t}_r) \\ \Delta b_r = \boldsymbol{\tau}_r^{\text{T}} ((b_r \mathbf{I} - \mathbf{F}_2) \Delta \mathbf{t}_r - \Delta \mathbf{F}_2 \mathbf{t}_r) \end{cases} \quad (16)$$

IV. SINGLE-TONE CASE

In this section, we calculate the perturbations of the parameter estimates for the signal $y(m_1, m_2) = ca^{m_1} b^{m_2}$.

A. Basic expressions

Let \mathbf{u} be the left singular vector of the signal subspace. Then (5) is rewritten as

$$\mathbf{F}_1 = \mathbf{u} \mathbf{u}^{\text{H}}, \quad \mathbf{F}_2 = \mathbf{u} \mathbf{u}^{\text{H}}. \quad (17)$$

Since, for a single tone, \mathbf{F}_1 and \mathbf{F}_2 are just scalars, we have that $a = \mathbf{F}_1$ and $b = \mathbf{F}_2$, from which it follows that

$$\begin{cases} \Delta a = \frac{1}{\|\mathbf{u}\|^2} \mathbf{u}^{\text{H}} (\Delta \mathbf{u} - a \Delta \mathbf{u}), \\ \Delta b = \frac{1}{\|\mathbf{u}\|^2} \mathbf{u}^{\text{H}} (\Delta \mathbf{u} - b \Delta \mathbf{u}). \end{cases} \quad (18)$$

Let $c = |c|e^{j2\pi\phi}$. Then an SVD of \mathbf{H} , $\sigma\mathbf{u}\mathbf{v}^H$, is given by

$$\sigma = |c|\sqrt{h_u h_v},$$

$$\mathbf{u} = \frac{e^{j2\pi\phi}}{\sqrt{h_u}} \left(\mathbf{a}^{(L_1)} \boxtimes \mathbf{b}^{(L_2)} \right), \mathbf{v} = \frac{1}{\sqrt{h_v}} \left(\mathbf{a}^{*(K_1)} \boxtimes \mathbf{b}^{*(K_2)} \right),$$

$$h_u = \|\mathbf{a}^{(L_1)}\|^2 \|\mathbf{b}^{(L_2)}\|^2, \quad h_v = \|\mathbf{a}^{(K_1)}\|^2 \|\mathbf{b}^{(K_2)}\|^2,$$

where for $x \in \mathbb{C}$ we define $\mathbf{x}^{(L)} = [1, x, \dots, x^{(L-1)}]^T$, $(*)$ denotes the elementwise conjugation, and \boxtimes is the Kronecker product of matrices (vectors are one-column matrices).

B. Expressions for the first-order perturbations

Now, by replacing expressions in (18) by the first-order perturbation (9), we obtain

$$\begin{aligned} \Delta a &= \frac{1}{\sigma \|\underline{\mathbf{u}}\|^2} \underline{\mathbf{u}}^H (\overline{\mathbf{I}} - a_1 \underline{\mathbf{I}}) \mathbf{U}_n \mathbf{U}_n^H \Delta \mathbf{H} \mathbf{v} \\ &= \frac{1}{\sigma \|\underline{\mathbf{u}}\|^2} \left(\underline{\mathbf{u}}^H (\overline{\mathbf{I}} (\mathbf{I} - \mathbf{u}\mathbf{u}^H) - a_1 \underline{\mathbf{I}} (\mathbf{I} - \mathbf{u}\mathbf{u}^H)) \Delta \mathbf{H} \mathbf{v} \right) \\ &= \frac{1}{\sigma \|\underline{\mathbf{u}}\|^2} \left(\underline{\mathbf{u}}^H (\overline{\mathbf{I}} - \overline{\mathbf{u}}\mathbf{u}^H - a_1 \underline{\mathbf{I}} + \overline{\mathbf{u}}\mathbf{u}^H) \Delta \mathbf{H} \mathbf{v} \right) \\ &= \frac{1}{\sigma \|\underline{\mathbf{u}}\|^2} \left(\underline{\mathbf{u}}^H (\overline{\mathbf{I}} - a_1 \underline{\mathbf{I}}) \Delta \mathbf{H} \mathbf{v} \right), \end{aligned}$$

where \mathbf{I} is the $L_1 L_2 \times L_1 L_2$ identity matrix.

Next, the matrices $\overline{\mathbf{I}}$ and $\underline{\mathbf{I}}$ can be first expressed as

$$\overline{\mathbf{I}} = \overline{\mathbf{I}}_{L_1} \boxtimes \mathbf{I}_{L_2} \quad \text{and} \quad \underline{\mathbf{I}} = \mathbf{I}_{L_1} \boxtimes \mathbf{I}_{L_2},$$

where under- and over-bars are defined in Section II. Hence, in particular

$$\underline{\mathbf{u}} = \frac{e^{j2\pi\phi}}{\sqrt{h_u}} (\mathbf{a}^{(L_1-1)} \boxtimes \mathbf{b}^{L_1}).$$

Second, since $\Delta \mathbf{H}$ is a Hankel-block-Hankel matrix for the noise term $e(m_1, m_2)$, the product $\Delta \mathbf{H} \mathbf{v}$ can be written as the two-dimensional convolution, which yields

$$\Delta \mathbf{H} \mathbf{v} = \frac{1}{\sqrt{h_v}} (\mathbf{G}_{a^*}^{(L_1, K_1)} \boxtimes \mathbf{G}_{b^*}^{(L_2, K_2)}) \mathbf{e},$$

where \mathbf{e} is the vectorized noise term

$$\mathbf{e} = [e(0, 0), \dots, e(0, M_2 - 1), \dots, e(M_1 - 1, 0), \dots, e(M_1 - 1, M_2 - 1)]^T,$$

and for x , the matrix $\mathbf{G}_x^{(L, K)}$ is the convolution matrix

$$\mathbf{G}_x^{(L, K)} = \begin{bmatrix} 1 & x & \dots & x^{K-1} & & \\ & \ddots & \ddots & \ddots & \ddots & \\ & & 1 & x & \dots & x^{K-1} \end{bmatrix} \in \mathbb{C}^{L \times (K+L-1)},$$

where the blank elements denote zeros. Hence,

$$\begin{aligned} \Delta a &= \frac{\|\mathbf{a}^{(L_1)}\|^2 e^{j2\pi\phi}}{\sigma \sqrt{h_v} \|\mathbf{a}^{L_1-1}\|^2} \frac{(\mathbf{a}^{(L_1-1)} \boxtimes \mathbf{b}^{L_1})^H}{\sqrt{h_u}} (\overline{\mathbf{I}}_{L_1} \boxtimes \mathbf{I}_{L_2})^T \\ &\cdot (\overline{\mathbf{I}}_{L_1} \boxtimes \mathbf{I}_{L_2} - a_1 \underline{\mathbf{I}}_{L_1} \boxtimes \mathbf{I}_{L_2}) (\mathbf{G}_{a^*}^{(L_1, K_1)} \boxtimes \mathbf{G}_{b^*}^{(L_2, K_2)}) \mathbf{e} \\ &= \frac{\|\mathbf{a}^{(L_1)}\|^2}{\sigma \sqrt{h_u h_v} \|\mathbf{a}^{(L_1-1)}\|^2} \\ &\left((\mathbf{a}^{(L_1-1)})^H (\overline{\mathbf{I}}_{L_1} - a_1 \underline{\mathbf{I}}_{L_1}) \mathbf{G}_{a^*}^{(L_1, K_1)} \right) \boxtimes \left((\mathbf{b}^{(L_1)})^H \mathbf{G}_{b^*}^{(L_2, K_2)} \right) \mathbf{e}. \end{aligned}$$

C. Expressions for the moments of the perturbations

Since \mathbf{e} is zero-mean, we have that $\mathbb{E}\{\Delta a\} = 0$. Next, since $\mathbb{E}\{\mathbf{e}\mathbf{e}^H\} = \mathbf{I}_{M_1 M_2}$, the variance of Δa can be expressed as

$$\mathbb{E}\{|\Delta a|^2\} = \frac{\sigma_e^2}{|c|^2} f(L_1, M_1, a) g(L_2, M_2, b), \quad (19)$$

where the functions $f(L, M, x)$ and $g(L, M, x)$ are defined as

$$\begin{aligned} f(L, M, x) &= \frac{\|(\mathbf{x}^{(L-1)})^H (\overline{\mathbf{I}}_L - x \underline{\mathbf{I}}_L) \mathbf{G}_{x^*}^{(L, K)}\|^2}{\|\mathbf{x}^{(K)}\|^4 \|\mathbf{x}^{(L-1)}\|^4}, \\ g(L, M, x) &= \frac{\|(\mathbf{x}^{(L)})^H \mathbf{G}_{x^*}^{(L, K)}\|^2}{\|\mathbf{x}^{(L)}\|^4 \|\mathbf{x}^{(K)}\|^4}, \end{aligned}$$

and $K = M - L + 1$. Similarly, we get

$$\mathbb{E}\{|\Delta b|^2\} = \frac{\sigma_e^2}{|c|^2} f(L_2, M_2, b) g(L_1, M_1, a). \quad (20)$$

It can be verified that the variances of the frequencies and the damping factors are deduced by:

$$\text{var}(\Delta\omega_a) = \text{var}(\Delta\alpha_a) = \frac{\mathbb{E}\{|\Delta a|^2\}}{2|a|^2} \quad (21)$$

$$\text{var}(\Delta\omega_b) = \text{var}(\Delta\alpha_b) = \frac{\mathbb{E}\{|\Delta b|^2\}}{2|b|^2}. \quad (22)$$

D. Closed form expressions

Our next goal is to give closed-form expressions of $f(L, M, x)$ and $g(L, M, x)$. It is easy to see that

$$\begin{aligned} (\mathbf{x}^{(L)})^H \mathbf{G}_{x^*}^{(L, K)} &= [1, 2x^*, 3x^{*2}, \dots, L_{2*} x^{*(L_*-1)}, \dots, \\ &L_* x^{*(M-L_*)}, (L_* - 1) x^{*(M-L_*+1)}, \dots, 2x^{M-2}, \dots, 1]. \end{aligned}$$

where $L_* = \min(L, K)$. Next, we have that

$$\begin{aligned} & [(\mathbf{x}^{(L-1)})^H (\overline{\mathbf{I}}_L - x \underline{\mathbf{I}}_L) \mathbf{G}_{x^*}^{(L, K)}]_i = \\ & \begin{cases} (i(1 - |x|^2) - |x|^2) x^{*(i-1)}, & i = 0, \dots, L_{**} - 1 \\ L_{**} (1 - |x|^2) x^{*(i-1)}, & i = L_{1*}, \dots, M - L_{**} - 1 \\ ((M - i)(1 - |x|^2) + |x|^2) x^{*(i-1)}, & i = M - L_{**}, \dots, M - 1 \end{cases} \end{aligned}$$

where $L_{**} = \min(L - 1, K)$. In the damped case ($|x| \neq 1$), after tedious calculations, Eq. (25) and (26) can be obtained for $f(L, M, x)$ and $g(L, M, x)$. In the undamped case the expressions are much simpler and are given in (23) and (24). We notice that the functions f and g are symmetric with respect to $L = \frac{M}{2} + 1$ and $L = \frac{M+1}{2}$, respectively.

$$f(L, M, x) = \begin{cases} \frac{2}{K^2(L-1)}, & \text{if } L - 1 \leq \frac{M}{2} \text{ and } |x| = 1 \\ \frac{2}{K(L-1)^2}, & \text{if } L - 1 \geq \frac{M}{2} \text{ and } |x| = 1 \end{cases} \quad (23)$$

$$g(L, M, x) = \begin{cases} \frac{1}{K} \left(1 - \frac{L^2-1}{3LK} \right), & \text{if } L \leq \frac{M+1}{2} \text{ and } |x| = 1 \\ \frac{1}{L} \left(1 - \frac{K^2-1}{3LK} \right), & \text{if } L \geq \frac{M+1}{2} \text{ and } |x| \neq 1 \end{cases} \quad (24)$$

$$\begin{aligned} f(L, M, x) &= (1 - |x|^2)^3 \times \\ & \begin{cases} \frac{1 + |x|^{2K}}{(1 - |x|^{2K})^2 (1 - |x|^{2(L-1)})}, & \text{if } L - 1 \leq \frac{M}{2} \text{ and } |x| \neq 1 \\ \frac{1 + |x|^{2(L-1)}}{(1 - |x|^{2K})(1 - |x|^{2(L-1)})^2}, & \text{if } L - 1 \geq \frac{M}{2} \text{ and } |x| \neq 1 \end{cases} \end{aligned} \quad (25)$$

$$g(L, M, x) = (1 - |x|^2) \times \begin{cases} \frac{-2L(1-|x|^2)(|x|^{2K} + |x|^{2L})}{(1-|x|^{2L})^2(1-|x|^{2K})^2} + \frac{(1+|x|^{2K})(1+|x|^2)}{(1-|x|^{2L})(1-|x|^{2K})^2}, & \text{if } L \leq \frac{M+1}{2} \text{ and } |x| \neq 1 \\ \frac{-2K_2(1-|x|^2)(|x|^{2L} + |x|^{2K})}{(1-|x|^{2L})^2(1-|x|^{2K})^2} + \frac{(1+|x|^{2L})(1+|x|^2)}{(1-|x|^{2L})^2(1-|x|^{2K})}, & \text{if } L \geq \frac{M+1}{2} \text{ and } |x| \neq 1 \end{cases} \quad (26)$$

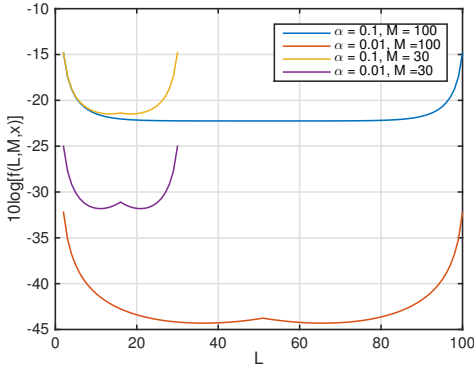


Fig. 1. Behavior of function $f(L, M, x)$ as a function of L for different values of M and damping factors.

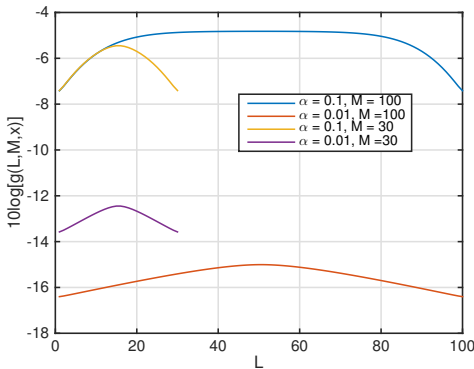


Fig. 2. Behavior of function $g(L, M, x)$ as a function of L for different values of M and damping factors.

E. Optimal values for L_1 and L_2

In [13], the optimal value of L has been obtained so as to minimize the variances of estimated parameters. In the case of 2-D ESPRIT, there are two variables, L_1 and L_2 , but they separate in the expressions of variances. Therefore, the optimal values of L_1 and L_2 are simply given by minimal values of each function, namely f and g .

As discussed in [13], the optimal L for $f(L, M, x)$ lies between $M/3$ and $M/2$ and approaches $M/2$ as the damping factor of x increases (or if M tends to ∞). These results are shown in Figure 1. Regarding function $g(L, M, x)$, it can be seen from Figure 2 that the minimum is reached for small L . Therefore, the optimal values of L_1 and L_2 minimizing $\text{var}(\Delta\omega_a)$ (resp. $\text{var}(\Delta\omega_b)$) lie between $M/3$ and $M/2$ for L_1 (resp. L_2) and are small for L_2 (resp. L_1). This is illustrated by typical examples in Figure 3 (resp. Figure 4). As in [7], the total Mean Square Error (tMSE) is taken to be $\text{MSE} = \text{var}(\Delta\omega_a) + \text{var}(\Delta\omega_b)$; the tMSE corresponding to Figures 3-4 is plotted in Figure 5.

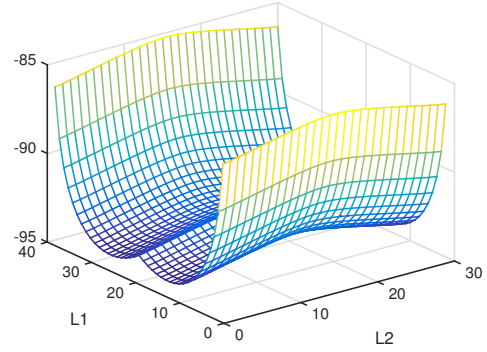


Fig. 3. Variance of $\Delta\omega_a$ as a function of L_1 and L_2

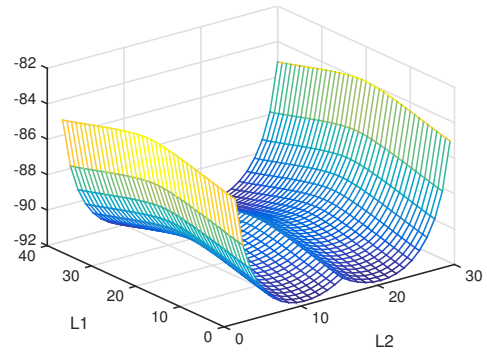


Fig. 4. Variance of $\Delta\omega_b$ as a function of L_1 and L_2

V. SIMULATIONS

We consider a 2-D damped single-tone signal with parameters $(\alpha_a, \omega_a) = (-0.1, 0.2\pi)$ and $(\alpha_b, \omega_b) = (-0.1, 0.4\pi)$. The SNR is fixed to 40 dB. Figure 6 shows the sample MSE and its theoretical value for ω_1 obtained from 200 Monte Carlo trials with $(M_1, M_2) = (30, 30)$. Since it is difficult to see the difference between the two curves in a 3-D plot, we show only one slice of the 3-D plot corresponding to $L_2 = 4$. We can observe that the theoretical MSEs are close to the estimated ones. In the second example, we repeat the same experience with $(M_1, M_2) = (100, 100)$ using the fast SVD method. The obtained results are reported in Figure 7, where it can be seen that theoretical MSEs are again close to the estimated ones.

In the third example, the same parameters of the modes are used but the SNR is varying. The parameters (L_1, L_2) are set to $(4, 4)$. The obtained results are depicted in Figure 8. We observe that the theoretical results are almost equal to empirical ones beyond a threshold, which is here -5 dB.

To compute 2D-ESPRIT estimates, we use the fast methods for partial SVD of Hankel-block-Hankel matrices [14, Sec. 6], where only the first R singular values/vectors are computed. The overall complexity of 2D-ESPRIT becomes $O(FM \log M)$ flops, compared with the complexity $O(L^2 K)$ of the naive implementation (where $K = K_1 K_2$, $L = L_1 L_2$

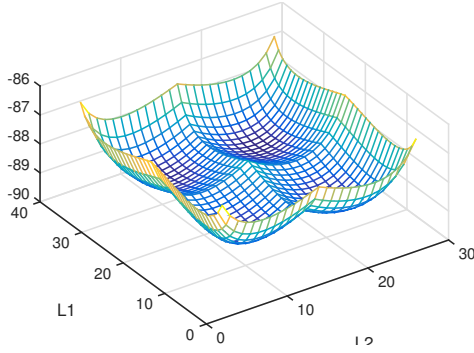


Fig. 5. tMSE as a function of L_1 and L_2

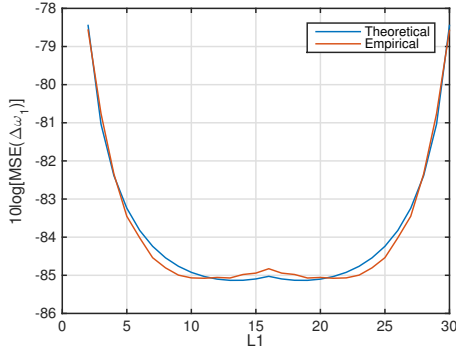


Fig. 6. Theoretical and empirical MSEs for 2-D ESPRIT versus L_1 , ($L_2 = 4$). $(\alpha_a, \omega_a) = (-0.1, 0.2\pi)$, $(\alpha_b, \omega_b) = (-0.1, 0.4\pi)$, $(M_1, M_2) = (30, 30)$, SNR = 40 dB.

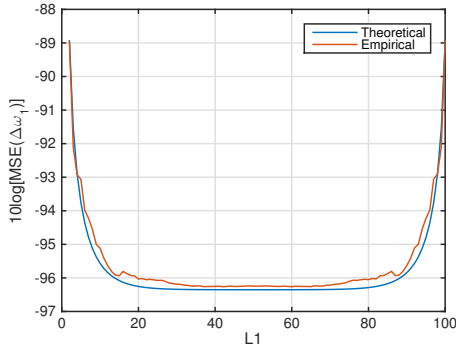


Fig. 7. Theoretical and empirical MSEs for 2-D ESPRIT (fast SVD) versus L_1 , ($L_2 = 4$). $(\alpha_a, \omega_a) = (-0.1, 0.2\pi)$, $(\alpha_b, \omega_b) = (-0.1, 0.4\pi)$, $(M_1, M_2) = (100, 100)$, SNR = 40 dB.

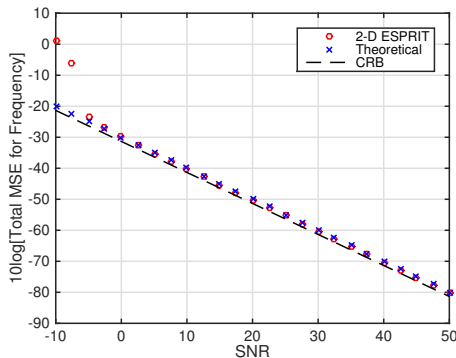


Fig. 8. Theoretical and empirical tMSEs for 2-D ESPRIT versus SNR. $(L_1, L_2) = (4, 4)$. $(\alpha_a, \omega_a) = (-0.1, 0.2\pi)$, $(\alpha_b, \omega_b) = (-0.1, 0.4\pi)$, $(M_1, M_2) = (10, 10)$.

and $M = M_1 M_2$). Hence, optimal or near-optimal values of parameters (for example, $(L_1, L_2) = (M_1/2, M_2/2)$) can be used for large signals.

VI. CONCLUSION

The 2-D ESPRIT algorithm is implemented by storing the $M_1 \times M_2$ data matrix into a HbH matrix with $L_1 L_2$ lines. A perturbation analysis has been carried out, which led to a closed form expression of the variances of parameters (damping factors and frequencies). It has then been shown that variables L_1 and L_2 separate in each of these variances. Our conclusion is that, for applications where damping factors are known to be less than 0.1, the optimal values of L_i should be chosen in the interval $[M_i/4, M_i/2]$. In the general case, *i.e.*, in the absence of *a priori* on damping factors, the optimal values of L_i may be chosen in $[2, M_i/2]$.

REFERENCES

- [1] J. Sacchini, W. Steedly, and R. Moses, "Two-dimensional Prony modeling and parameter estimation," *IEEE Trans. Signal Process.*, vol. 41, no. 11, pp. 3127–3137, 1993.
- [2] Y. Hua, "Estimating two-dimensional frequencies by matrix enhancement and matrix pencil," *IEEE Trans. Signal Process.*, vol. 40, no. 9, pp. 2267–2280, 1992.
- [3] S. Rouquette and M. Najim, "Estimation of frequencies and damping factors by two-dimensional ESPRIT type methods," *IEEE Trans. Signal Process.*, vol. 49, no. 1, pp. 237–245, 2001.
- [4] K. Mokios, N. Sidiropoulos, M. Pesavento, and C. Mecklenbrauker, "On 3-D harmonic retrieval for wireless channel sounding," in *Proc. IEEE ICASSP*, Montreal, Canada, May 2004, pp. ii89–ii92.
- [5] J. Liu and X. Liu, "An eigenvector-based approach for multidimensional frequency estimation with improved identifiability," *IEEE Trans. Signal Process.*, vol. 54, no. 12, pp. 4543–4556, 2006.
- [6] J. Liu, X. Liu, and X. Ma, "Multidimensional frequency estimation with finite snapshots in the presence of identical frequencies," *IEEE Transactions on Signal Processing*, vol. 55, pp. 5179–5194, 2007.
- [7] M. Haardt, F. Roemer, and G. Del Galdo, "Higher-order SVD-based subspace estimation to improve the parameter estimation accuracy in multidimensional harmonic retrieval problems," *IEEE Trans. Signal Process.*, vol. 56, no. 7, pp. 3198–3213, 2008.
- [8] L. Huang, Y. Wu, H. So, Y. Zhang, and L. Huang, "Multidimensional sinusoidal frequency estimation using subspace and projection separation approaches," *IEEE Trans. Signal Process.*, vol. 60, no. 10, pp. 5536–5543, 2012.
- [9] C. Lin and W. Fang, "Efficient multidimensional harmonic retrieval: A hierarchical signal separation framework," *IEEE Signal Process. Lett.*, vol. 20, no. 5, pp. 427–430, May 2013.
- [10] F. Roemer, M. Haardt, and G. Del Galdo, "Analytical performance assessment of multi-dimensional matrix- and tensor-based esprit-type algorithms," *IEEE Trans. Signal Process.*, vol. 62, no. 10, pp. 2611–2625, 2014.
- [11] F. Li, H. Liu, and R. J. Vaccaro, "Performance analysis for doa estimation algorithms: unification, simplification, and observations," *Aerospace and Electronic Systems, IEEE Transactions on*, vol. 29, no. 4, pp. 1170–1184, 1993.
- [12] Z. Xu, "Perturbation analysis for subspace decomposition with applications in subspace-based algorithms," *IEEE Trans. Signal Process.*, vol. 50, no. 11, pp. 2820–2830, 2002.
- [13] E.-H. Djermoune and M. Tomczak, "Perturbation analysis of subspace-based methods in estimating a damped complex exponential," *IEEE Trans. Signal Process.*, vol. 57, no. 11, pp. 4558–4563, 2009.
- [14] N. Golyandina, A. Korobeynikov, A. Shlemov, and K. Usevich, "Multivariate and 2D extensions of Singular Spectrum Analysis with the Rssa package," *Journal of Statistical Software*, vol. 67, no. 1, 2015.